







ORIGINAL RESEARCH

Short-Term Changes in Left and Right Ventricular Cardiac Magnetic Resonance Feature Tracking Strain Following Ferric Carboxymaltose in Patients With Heart Failure: A Substudy of the Myocardial-IRON Trial

Irene del Canto, PhD*; Enrique Santas, MD, PhD*; Ingrid Cardells, MD, PhD; Gema Miñana, MD, PhD; Patricia Palau, MD, PhD; Pau Llàcer, MD, PhD; Lorenzo Fácila, MD, PhD; Raquel López-Vilella, MD; Luis Almenar, MD, PhD; Vicent Bodí , MD, PhD; Maria P. López-Lereu, MD, PhD; Jose V. Monmeneu, MD, PhD; Juan Sanchis , MD, PhD; David Moratal , PhD; Alicia M. Maceira , MD, PhD; Rafael de la Espriella, MD; Francisco J. Chorro, MD, PhD; Antoni Bayés-Genís , MD, PhD; Julio Núñez , MD, PhD; on behalf of Myocardial-IRON Investigators[†]

BACKGROUND: The mechanisms explaining the clinical benefits of ferric carboxymaltose (FCM) in patients with heart failure, reduced or intermediate left ventricular ejection fraction, and iron deficiency remain not fully clarified. The Myocardial-IRON trial showed short-term cardiac magnetic resonance (CMR) changes suggesting myocardial iron repletion following administration of FCM but failed to find a significant increase in left ventricular ejection fraction in the whole sample. Conversely, the strain assessment could evaluate more specifically subtle changes in contractility. In this subanalysis, we aimed to evaluate the effect of FCM on the short-term left and right ventricular CMR feature tracking derived strain.

METHODS AND RESULTS: This is a post hoc subanalysis of the double-blind, placebo-controlled, randomized clinical trial that enrolled 53 ambulatory patients with heart failure and left ventricular ejection fraction <50%, and iron deficiency [Myocardial-IRON trial (NCT03398681)]. Three-dimensional left and 2-dimensional right ventricular CMR tracking strain (longitudinal, circumferential, and radial) changes were evaluated before, 7 and 30 days after randomization using linear mixed-effect analysis. The median (interquartile range) age of the sample was 73 years (65–78), and 40 (75.5%) were men. At baseline, there were no significant differences in CMR feature tracking strain parameters across both treatment arms. At 7 days, the only global 3-dimensional left ventricular circumferential strain was significantly higher in the FCM treatment-arm (difference: -1.6%, $P=0.001$). At 30 days, and compared with placebo, global 3-dimensional left ventricular strain parameters significantly improved in those allocated to FCM treatment-arm [longitudinal (difference: -2.3%, $P<0.001$), circumferential (difference: -2.5%, $P<0.001$), and radial (difference: 4.2%, $P=0.002$)]. Likewise, significant improvements in global right ventricular strain parameters were found in the active arm at 30 days (longitudinal [difference: -3.3%, $P=0.010$], circumferential [difference: -4.5%, $P<0.001$], and radial [difference: 4.5%, $P=0.027$]).

CONCLUSIONS: In patients with stable heart failure, left ventricular ejection fraction <50%, and iron deficiency, treatment with FCM was associated with short-term improvements in left and right ventricular function assessed by CMR feature tracking derived strain parameters.

REGISTRATION: URL: <https://www.clinicaltrials.gov>; Unique identifier: NCT03398681.

Correspondence to: Julio Núñez, MD, PhD, Cardiology Department, Hospital Clínico Universitario de Valencia, Universitat de Valencia, INCLIVA, Valencia, Spain. Email: juenuvi@uv.es or yulnunez@gmail.com

*I. del Canto and E. Santas contributed equally.

[†]A complete list of the Myocardial-IRON Investigators can be found in the Appendix at the end of the article.

Supplemental Material for this article is available at <https://www.ahajournals.org/doi/suppl/10.1161/JAHA.121.022214>

For Sources of Funding and Disclosures, see page 11.

© 2022 The Authors. Published on behalf of the American Heart Association, Inc., by Wiley. This is an open access article under the terms of the Creative Commons Attribution-NonCommercial-NoDerivs License, which permits use and distribution in any medium, provided the original work is properly cited, the use is non-commercial and no modifications or adaptations are made.

JAHA is available at: www.ahajournals.org/journal/jaha

Key Words: CMR feature tracking ■ ferric carboxymaltose ■ heart failure ■ iron deficiency ■ ventricular strain

CLINICAL PERSPECTIVE

What Is New?

- In patients with iron deficiency and heart failure and reduced ejection fraction, this study showed that treatment with iron ferric carboxymaltose translated into a significant short-term improvement in left and right systolic function assessed by cardiac magnetic resonance feature tracking–derived strain parameters.

What Are the Clinical Implications?

- These findings endorse the utility of treatment with iron ferric carboxymaltose in patients with iron deficiency and heart failure and reduced ejection fraction providing new evidence about the cardiac mechanisms explaining the clinical benefits of iron repletion in heart failure.

Nonstandard Abbreviations and Acronyms

CMR-FT	cardiac magnetic resonance feature tracking
FCM	ferric carboxymaltose
ID	iron deficiency
3D-GCS	3D-global circumferential strain
3D-GLS	3D-global longitudinal strain
3D-GRS	3D-global radial strain
2D-GCS	2D-global circumferential strain
2D-GLS	2D-global longitudinal strain
2D-GRS	2D-global radial strain

Iron deficiency (ID) is a common condition in patients with heart failure (HF), and it is associated with reduced functional capacity and an increased risk of hospitalizations and mortality.^{1–3} Treatment with intravenous ferric carboxymaltose (FCM) has been shown to improve quality of life and reduce the risk of HF hospitalizations in patients with chronic HF with reduced ejection fraction.^{4–6} This benefit has recently been expanded to patients hospitalized for acute HF.⁷ However, the mechanisms underlying such benefits remain not completely understood.^{8,9} Different preclinical studies showed adverse effects of ID on mitochondrial function among myoblasts and cardiomyocytes.^{10,11} Despite the growing research in this field, there is little clinical evidence on iron therapy's

impact on cardiac remodeling or ventricular function. The Myocardial-IRON trial showed that treatment with FCM causes short-term changes in cardiac magnetic resonance (CMR) sequences suggestive of myocardial iron repletion in patients with chronic HF and ID.¹² However, in this trial, we failed to find a significant increase in left ventricular ejection fraction (LVEF) in the whole sample.¹² Ejection fraction has its caveats when evaluating the systolic function, as it is affected by heart rate, loading conditions, and cardiac geometry.¹³ Nowadays, more accurate imaging-based techniques, such as myocardial strain analyses, can evaluate more specifically subtle changes in contractility.¹³ In fact, global myocardial function quantified by left ventricular (LV) strain using CMR has been shown to be an independent prognostic factor in patients with HF.^{14,15} CMR feature tracking (CMR-FT) is a novel and non-invasive technique with high accuracy and reproducibility for quantitatively assessing myocardial deformation.^{16,17} In this post hoc analysis of the Myocardial-IRON trial, we aimed to evaluate the association between treatment with FCM with early short-term changes in CMR-FT deformation parameters in patients with chronic HF and ID.

METHODS

Study Sample and Trial Intervention

The data that support the findings of this study are available from the corresponding author upon reasonable request. This is a post hoc analysis of an investigator-initiated, multicenter, randomized, double-blind, placebo-controlled clinical trial designed to evaluate the effect of intravenous FCM versus placebo on myocardial iron repletion estimated by T2* and T1 mapping CMR sequences, in patients with stable chronic HF (New York Heart Association class II and III), with systolic dysfunction (LVEF <50%), and ID (serum ferritin <100 µg/L or 100–299 µg/L with transferrin saturation <20%). Inclusion and exclusion criteria are reported elsewhere.¹⁸ The trial (NCT03398681) was conducted in 5 academic centers in Spain. Patients were randomized 1:1 to receive either FCM or placebo. FCM (Ferinject, Vifor Pharma, Glattbrugg, Switzerland) was given intravenously as perfusion of 20 mL solution (equivalent to 1000 mg of iron) diluted in a sterile saline solution (0.9% NaCl) administered over at least 15 minutes. In the placebo group, an intravenous saline solution (0.9% weight/volume NaCl) was administered over the same time. At 30 days, patients assigned to placebo received intravenous FCM if ID persisted. The

study design and main results were previously published. From May 2017 to June 2018, a total of 53 patients were randomly assigned to receive FCM (n=27) or placebo (n=26).¹² Characteristics of the study sample were defined according to established definitions.¹⁹⁻²¹

The investigation conforms to the principles outlined in the Declaration of Helsinki and Good Clinical Practice of the International Conference on Harmonization. The study protocol was approved by the Spanish Agency for Medicines and Medical Devices and by Clinical Research Ethics Committee of the University Clinical Hospital of Valencia. All patients signed and dated the informed consent form.

Cardiac Magnetic Resonance

CMR studies were performed by 2 experienced operators (M.P.L.L., 21 years of CMR training, and J.V.M.M., 15 years of CMR training, both with European Association of Cardiovascular Imaging-CMR level 3) on a 1.5 Tesla MR scanner (Essenza and Avanto, Siemens, Erlangen, Germany) using the spine and phased array 6-channel surface coils. All images were obtained with electrocardiographic gating and breath-holding. Cine sequences in the 2-, 3-, and 4-chamber views were obtained. Also, contiguous short-axis cine from the atrioventricular plane to the apex were acquired at rest every 1 cm with steady-state free precession imaging sequences. Detailed sequences parameters are provided in Table S1. Typically, 40 shared phases were acquired in each cine sequence, and the temporal resolution was 37 ms.

Cine images were analyzed offline by 2 experienced observers masked to all patient data using customized software (QMASS-MR 6.1.5, Medis, Leiden, Netherlands). Right ventricular (RV) ejection fraction and LVEF, LV end-diastolic and end-systolic volume index (mL/m²), and LV mass (g/m²) were quantified by semiautomatic planimetry of endocardial and epicardial borders in short-axis-view cine images.

The basic T2* pulse sequence is a breath-hold, multi-echo gradient-echo T2* sequence (voxel size: 1.6×1.6×8 mm) with 8 echo times from 2.65 to 21 ms, in the mid-ventricular short axis. For T2* analysis, a region of interest was chosen in the mid-LV septum. The mean signal intensities of the regions of interest were measured in the series of increasing echo time images to give an exponential decay curve. The monoexponential decay model and the non-linear curve fitting algorithm were used to fit the curve to obtain T2* measurement.

Feature Tracking Analysis

For strain analysis, the 2-dimensional (2D) and 3-dimensional (3D) feature tracking analyses were performed by the same operator masked to treatment

allocation. The cine steady-state free precession images were processed and analyzed using a dedicated magnetic resonance feature tracking software package (CVI42, Circle Cardiovascular Imaging, Canada). At end-diastole, LV endocardial and epicardial boundaries were manually delineated in the 2-, 3-, 4-chamber, and short-axis views, excluding papillary muscles from the endocardial contour. Likewise, RV endocardial and epicardial boundaries were delineated in the 4-chamber and short-axis views. The superior and inferior right ventricular insertion points were additionally defined on short-axis cines. Then, in the 2-, 3-, and 4-chamber view images, a straight line from the midpoint of the mitral annular plane to the apex was depicted (Figure 1A through 1D). Finally, an automated tracking algorithm was applied to propagate the contours throughout the cardiac cycle, and the rendered contours were reviewed and adjusted in case of inadequate automatic border tracking.

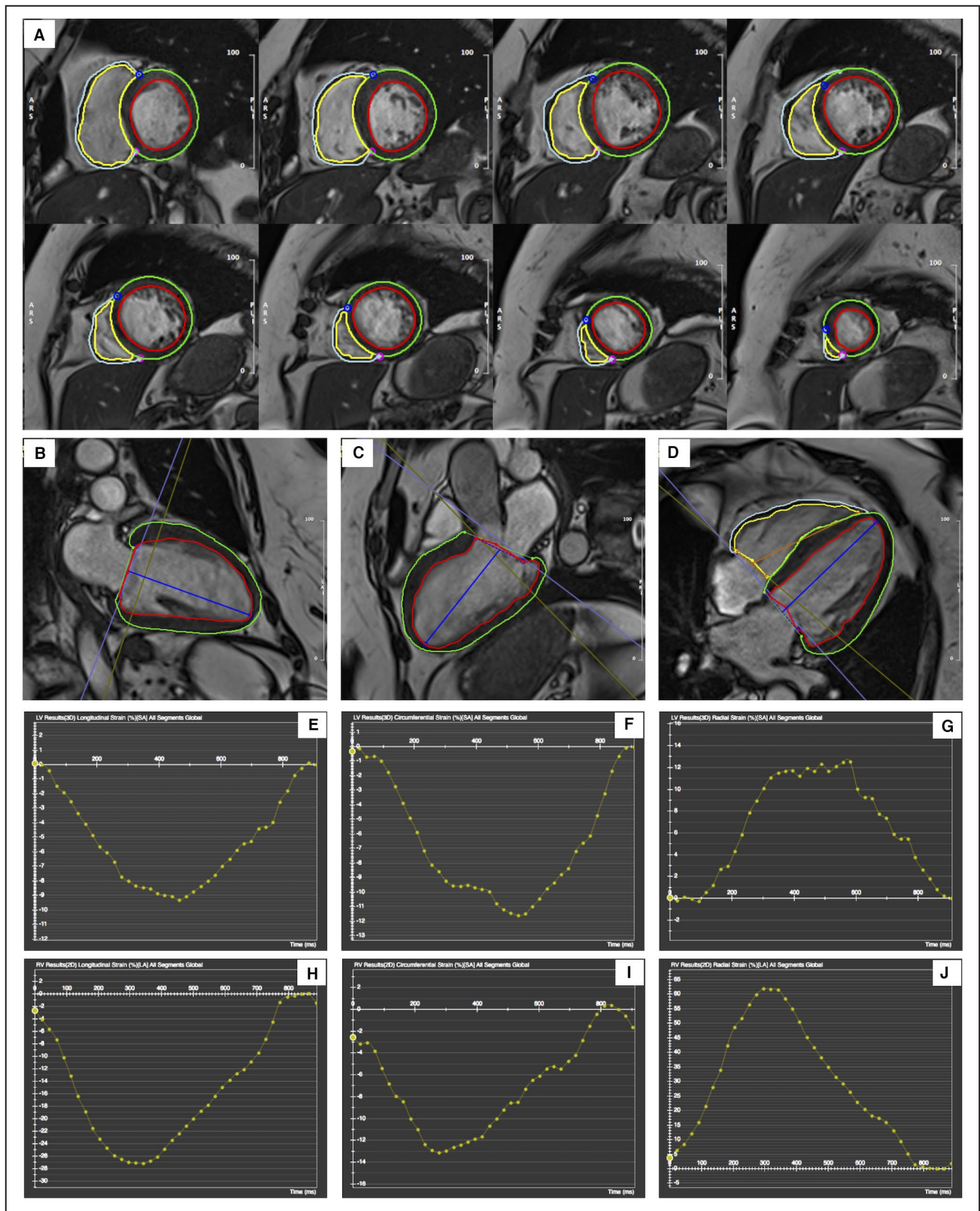
The algorithm performs an automatic strain analysis (automatically computed in all slices that contain endo- and epicardial contours). In particular, the 2D algorithm fits a 2D incompressible deformable model of the myocardium to individual image slices (eg, long or short axis acquisitions) over the cardiac cycle.²² In this 2D-analysis, long-axis cines were tracked to derive longitudinal strain parameters, and short-axis cines were used to derive circumferential and radial strain parameters.

Additionally, the 3D algorithm fits a 3D deformable model of the myocardium between the endocardial and epicardial surfaces generated by interpolating the tracked boundaries from the 2D algorithm. The surface interpolation is performed using both long and short-axis image information, which makes it suitable for inferring the radial, circumferential, and longitudinal motions of the myocardium.²²

Finally, the analysis was performed over the entire cardiac cycle, resulting in a strain-time curve (Figure 1E through 1J); 2D and 3D global radial peak systolic strain (GRS), global circumferential peak systolic strain (GCS), and global longitudinal peak systolic strain (GLS) were obtained as the maximum strain magnitude on the strain curve.

End Points

The end points of this subanalysis were changes in LV and RV cardiac deformation parameters assessed by CMR-FT at 7 and 30 days. We selected 3D strain parameters for LV deformation because 3D CMR-FT offers better accuracy and reproducibility, reducing artifacts from through-plane motion presented in 2D analysis.^{16,23} Therefore, 3D-GLS, 3D-GCS, and 3D-GRS were evaluated for LV. For RV deformation, we opted for 2D CMR-FT analysis, which has excellent



intra- and inter-observer agreement, rather than 3D because the RV only appears in 4-chamber view, and 3D analysis would decrease the accuracy in strain quantification.²⁴ Thus, for RV, 2D-GLS, 2D-GCS, and 2D-GRS

were assessed. An exploratory analysis included the association between LV CMR-FT strain parameters (3D-GLS, 3D-GCS, and 3D-GRS) and changes in T2* (CMR-surrogate of myocardial iron content).²⁵

Downloaded from <http://ahajournals.org> by on April 11, 2022

Figure 1. Left ventricular (LV) and right ventricular (RV) cardiac magnetic resonance feature tracking in the short-axis (A), and 2-chamber (B), 3-chamber (C), and 4-chamber (D) cine images at end-diastole.

The red and green curves delineate the endocardial and epicardial contours in LV, respectively; the yellow and cyan curves delineate the endocardial and epicardial contours in the RV, respectively. The blue and magenta points represent the superior and inferior RV insertion points on short-axis cines (A). The blue (LV) and orange (RV) lines are used to define the base and apex of the mitral annulus plane and the apical plane (B through D). Representation of LV global longitudinal strain, global circumferential strain, and global radial strain curves using 3D cardiac magnetic resonance feature tracking (E through G). Representation of RV global longitudinal strain, global circumferential strain, and global radial strain curves using 2D cardiac magnetic resonance feature tracking (H through J).

Assessment of Reproducibility

Inter-observer reproducibility for the measurement of CMR-FT LV and RV strains was assessed in 16 CMR studies (30%) randomly selected from the study group. For this purpose, the differences between the measurements performed by the 2 operators using the dedicated magnetic resonance feature tracking software package (CVI42, Circle Cardiovascular Imaging, Canada) were determined.

Statistical Analysis

All statistical comparisons were performed under the intention-to-treat principle using Stata 15.1 (Stata Statistical Software, College Station, TX, USA). Observed mean values across treatment allocation were reported and compared using the paired *t*-test. The correlations among changes in strain parameters and changes in T2*, transferrin saturation (TSAT), and ferritin were evaluated by the Spearman test. Inter-observer reliability of measurements was assessed by calculating, for each parameter, the correlation between any 2 measurements made on the same subject by an absolute agreement 2-way random effects model intraclass correlation coefficient. Intraclass correlation coefficient estimates and their 95% CI were reported. Linear mixed effect models were used to evaluate the primary and exploratory end points. All analyses were adjusted for age, sex, hospital (as a cluster variable), the main term for treatment, the main term for visit, and the interaction term treatment*visit (7- and 30-day), and the baseline value of the regressed outcome. No adjustment was made for multiple comparisons. Results from the linear mixed effect models are presented as least square means with their respective 95% CIs and *P* values. All fixed-effects regression estimates were added in Tables S2 and S3. The proportion of missing values in CMR strain parameters were low (<5% for most of the parameters), and no imputations were performed.²⁶ All analyses were performed using Stata 15.1 (Stata Statistical Software, College Station, TX). A 2-sided *P* value of 0.05 was considered significant for all the analyses.

RESULTS

The study population's median age was 73 years (interquartile range, 65–78), and 40 (75.5%) were men. Ischemic etiology was present in 26 patients (49%), and

most (94.3%) were in New York Heart Association Class II. The median of NT-proBNP (N-terminal pro-B-type natriuretic peptide) at randomization was 1690 pg/mL (1010–2828). At baseline, all patients exhibited ID, and the median of ferritin and transferrin saturation (TSAT) were 63 µg/L (p25%–p75%: 33–114) and 15.7% (p25%–p75%: 11–19.2). The mean LVEF and RV ejection fraction in the whole sample were 40%±10% and 56%±11%, respectively. The patients' detailed baseline characteristics in the 2 study groups have been reported elsewhere without significant differences between treatment groups.¹² The means±SDs of LV strain parameters in the whole cohort were –5.6%±4.1%, –9.1%±3.5%, and 13.5%±5.2%, for LV 3D-GLS, LV 3D-GCS, and LV 3D-GRS, respectively. For RV parameters, the means±SDs for RV 2D-GLS, RV 2D-GCS, and RV 2D-GRS were: –13.4%±5.4%, –9.5%±4.5%, and 16.5%±9.7%, respectively. Clinical characteristics across treatment arms are presented in Table 1. There were no baseline differences in LVEF and RV ejection fraction across treatment arms (Table 1). Likewise, LV (3D-GLS, 3D-GCS, and 3D-GRS) and RV (2D-GLS, 2D-GCS, and 2D-GRS) strain parameters did not significantly differ across both treatment arms (Table 1).

Iron Treatment and Changes in LV Strain by Cardiac Magnetic Resonance-Feature Tracking LV 3D-GLS

Raw data of LV 3D-GLS across treatment allocation are presented in Table 2. The inferential analysis showed that LV 3D-GLS did not significantly differ between FCM and placebo at 7 days (Figure 2A, *P*=0.226; 95% CI, –2.3 to 0.4). Conversely, at 30 days, LV 3D-GLS significantly improved in the FCM arm compared with placebo (difference: –2.3%; 95% CI, –3.8 to –0.8; *P*<0.001; Figure 2A).

LV 3D-GCS

The descriptive analysis showed that the observed means of LV 3D-GCS along the visits is presented in Table 2. The inferential analysis confirmed that least square means significantly improved at both time points in the active-arm (7 days: difference –1.6%; 95% CI, –2.7 to –0.5; *P*=0.001; and 30 days: difference –2.5%; 95% CI, –3.6 to –1.4; *P*<0.001) as shown in Figure 2B.

Table 1. Baseline Characteristics by Treatment Arm

Variables	Placebo (n=26)	IV (n=27)	P value
Demographics and medical history			
Age (y)	71 (67–79)	73.5 (64–77)	0.957
Male, n (%)	19 (73.1)	21 (77.8)	0.691
Hypertension, n (%)	19 (73.1)	22 (81.5)	0.465
Dyslipidemia, n (%)	16 (61.5)	18 (66.7)	0.697
Diabetes, n (%)	14 (53.8)	15 (55.6)	0.901
Former smoker, n (%)	16 (61.5)	15 (55.6)	0.659
Coronary artery disease, n	10 (38.5)	13 (48.1)	0.477
Admission for AHF in last year, n (%)	16 (61.5)	16 (59.3)	0.865
COPD, n (%)	6 (23.1)	7 (25.9)	0.810
CKD, n (%)	7 (26.9)	8 (29.6)	0.827
Stroke, n (%)	6 (23.1)	2 (7.4)	0.111
Peripheral artery disease, n	4 (15.4)	4 (14.8)	0.954
NYHA functional class, n			0.080
II	26 (100)	24 (88.9)	
III	0	3 (11.1)	
Vital signs			
Heart rate, bpm	68 (64–77)	73 (68–82)	0.262
SBP, mm Hg	125 (113–146)	117 (109–132)	0.142
ECG and echocardiography			
Atrial fibrillation, n (%)	14 (53.8)	10 (37.0)	0.219
LBBB, n (%)	6 (23.1)	6 (22.2)	0.941
CMR parameters			
LVEDVI, mL/m ²	122.1 (101.5–137.9)	107 (80.1–143.9)	0.109
LVESVI, mL/m ²	72.5 (55.1–87.6)	63.5 (40.6–84)	0.096
LVEDDI, mm/m ²	30.8 (28–33.5)	30.9 (26.9–31.9)	0.493
LVESDI, mm/m ²	23.1 (21.1–26.9)	23.7 (23.0–26.8)	0.648
LVEF, %	38.1 (10.6)	42.3 (9.9)	0.141
RVEF, %	56.8 (10.6)	55.8 (12.3)	0.743
LV 3D-GLS, %	–5.3 (3.5)	–5.8 (4.6)	0.668
LV 3D-GCS, %	–9.4 (3.7)	–8.8 (3.3)	0.493
LV 3D-GRS, %	12.8 (5.2)	14.1 (5.1)	0.387
RV 2D-GLS, %	–14.7 (5.4)	–12.2 (5.1)	0.087
RV 2D-GCS, %	–9.7 (3.7)	–9.3 (5.2)	0.728
RV 2D-GRS, %	16.5 (10.5)	16.4 (9.0)	0.994
Laboratory results			
Hemoglobin, g/dL	13.4 (12.7–14.6)	13.1 (11.9–13.4)	0.084
Anemia (WHO), n (%)	6 (23.1)	10 (37.0)	0.268
Transferrin saturation, %	15.4 (9.6–20.0)	15.7 (12.0–19.2)	0.790

(Continued)

Table 1. Continued

Variables	Placebo (n=26)	IV (n=27)	P value
Ferritin, ng/mL	47.8 (23.0–114.0)	73.0 (56.0–126.0)	0.072
Absolute iron deficiency, n (%)	19 (73.1)	18 (66.7)	0.611
eGFR, mL/min per 1.73 m ²	64.1 (48.9–79.3)	59.4 (50.0–71.3)	0.854
NT-proBNP, pg/mL	1213 (1010–2667)	1990 (976–2830)	0.505
Medical treatment			
Diuretics, n (%)	24 (92.3)	25 (92.6)	0.969
Beta-blockers, n (%)	21 (80.8)	25 (92.6)	0.204
ACEI, n (%)	6 (23.1)	7 (25.9)	0.810
ARB, n (%)	4 (15.4)	5 (18.5)	0.761
Sacubitril/Valsartan, n (%)	8 (30.8)	10 (37.0)	0.630
MRA, n (%)	16 (61.5)	12 (44.4)	0.213

Values expressed as mean (SD) and median (percentile 25% to percentile 75%). Categorical variables are presented as percentages. ACEI indicates angiotensin-converting enzyme inhibitors; AHF, acute decompensated heart failure; ARB, angiotensin II receptor blockers; CKD, chronic kidney disease; CKD-EPI, Chronic Kidney Disease Epidemiology Collaboration; CMR, cardiac magnetic resonance; COPD, chronic pulmonary obstructive disease; eGFR, estimated glomerular filtration rate assessed by CKD-EPI equation; LBBB, left bundle branch block; LVEDDI, left ventricle end-diastolic diameter index; LVESDI, left ventricle end-systolic diameter index; LVEDVI, left ventricle end-diastolic volume index; LVESVI, left ventricle end-systolic volume index; LVEF, left ventricular ejection fraction; LV 3D-GCS, left ventricle 3D-global circumferential strain; LV 3D-GLS, left ventricle 3D-global longitudinal strain; LV 3D-GRS, left ventricle 3D-global radial strain; MRA, mineralocorticoid receptor antagonist; NT-proBNP, N-terminal propeptide brain natriuretic peptide; NYHA, New York Heart Association; RVEF, right ventricular ejection fraction; RV 2D-GCS, right ventricle 2D-global circumferential strain; RV 2D-GLS, right ventricle 2D-global longitudinal strain; RV 2D-GRS, right ventricle 2D-global radial strain; SBP, systolic blood pressure; and WHO, World Heart Organization.

Definitions:

Absolute iron deficiency was defined as ferritin <100 ng/mL.¹⁹ World Health Organization criteria for anemia: adult male, hemoglobin 13 g/dL; adult, non-pregnant female, hemoglobin 12 g/dL; pregnant adult women, hemoglobin 11 g/dL.²⁰ Chronic kidney disease was defined as current or previous history of chronic kidney disease, captured as the current status. Chronic kidney disease is defined as either kidney damage or glomerular filtration rate <60 mL/min per 1.73 m² for ≥3 months.²¹ Coronary artery disease was defined as current or previous history of any of the following: (1) coronary artery stenosis ≥50% (by cardiac catheterization or other modality of direct imaging of the coronary arteries), (2) previous coronary artery by-pass surgery, (3) previous percutaneous coronary intervention, or (4) previous myocardial infarction.²¹ Prior myocardial infarction, was defined as the presence of any 1 of the following criteria: (1) pathological Q waves with or without symptoms in the absence of nonischemic causes, (2) imaging evidence of a region of loss of viable myocardium that is thinned and/or fails to contract, in the absence of a nonischemic cause, or (3) pathological findings of a prior myocardial infarction.²¹ Stroke was defined as an acute episode of focal or global neurological dysfunction caused by brain, spinal cord, or retinal vascular injury as a result of hemorrhage or infarction.²¹ Heart failure (HF) hospitalization was defined as an event where the patient is admitted to the hospital with a primary diagnosis of HF where the length of stay is at least 24 hours (or extends over a calendar date if the hospital admission and discharge times are unavailable), where the patient exhibits new or worsening symptoms of HF on presentation, has objective evidence of new or worsening HF, and receives initiation or intensification of treatment specifically for HF.²¹ Obstructive coronary artery disease was defined as being present in patients with ≥50% stenosis in any major epicardial vessel or branch vessel >2.0 mm in diameter.²¹

Table 2. Raw Data for CMR-FT Strain Parameters

CMR-FT strain (%)	Placebo (n=26)	IV (n=27)	P value
7-d visit			
LV 3D-GLS	-5.9±3.2	-7.1±2.6	0.178
LV 3D-GCS	-8.5±3.4	-9.6±3.3	0.256
LV 3D-GRS	11.4±4.6	14.0±5.7	0.073
RV 2D-GLS	-15.0±6.0	-14.5±5.1	0.755
RV 2D-GCS	-9.1±4.6	-10.2±4.4	0.353
RV 2D-GRS	14.9±6.9	15.9±9.7	0.642
30-d visit			
LV 3D-GLS	-6.4±3.1	-8.5±3.7	0.030
LV 3D-GCS	-9.4±3.8	-10.8±3.0	0.143
LV 3D-GRS	12.5±4.6	16.9±6.5	0.008
RV 2D-GLS	-15.2±5.4	-16.1±5.6	0.574
RV 2D-GCS	-7.9±6.1	-12.0±4.2	0.006
RV 2D-GRS	14.2±6.4	18.2±8.7	0.040

Values are expressed as mean±SD. CMR-FT indicates cardiac magnetic resonance feature tracking; LV 3D-GCS, left ventricle 3D-global circumferential strain; LV 3D-GLS, left ventricle 3D-global longitudinal strain; LV 3D-GRS, left ventricle 3D-global radial strain; RV 2D-GCS, right ventricle 2D-global circumferential strain; RV 2D-GLS, right ventricle 2D-global longitudinal strain; and RV 2D-GRS, right ventricle 2D-global radial strain.

LV 3D-GRS

Observed means of LV 3D-GRS in both treatment arms are presented in Table 2. At 7 days, we did not find a significant difference between both treatment arms (difference: 2.1%; 95% CI, -0.4 to 4.7; $P=0.118$). However, 3D-GRS was significantly higher in those treated with FCM at 30 days (difference: 4.2%; 95% CI, 1.4 to 7.0; $P=0.002$; Figure 2C).

Iron Treatment and Changes in RV Strain by Cardiac Magnetic Resonance Feature Tracking

RV 2D-GLS

Raw data of RV 2D-GLS across treatment allocation are presented in Table 2. The inferential analysis revealed that this parameter did not significantly improve at 7 days (difference: -1.1%; 95% CI, -3.3 to 1.2; $P=0.483$), but it was significant at 30 days (difference: -3.3%; 95% CI, -5.9 to -0.7; $P=0.010$). Figure 3A shows the least square means (95% CI) across treatment arms at 2-time points.

RV 2D-GCS

Table 2 showed the observed means of RV 2D-GCS and 7 and 30 days. No significant changes in least square means of RV 2D-GCS were found at 7 days (difference: -1.1%; 95% CI, -2.7 to 0.6; $P=0.270$), but it improved significantly at 30 days (difference: -4.5%; 95% CI, -7.1 to -1.9; $P<0.001$) as shown in Figure 3B.

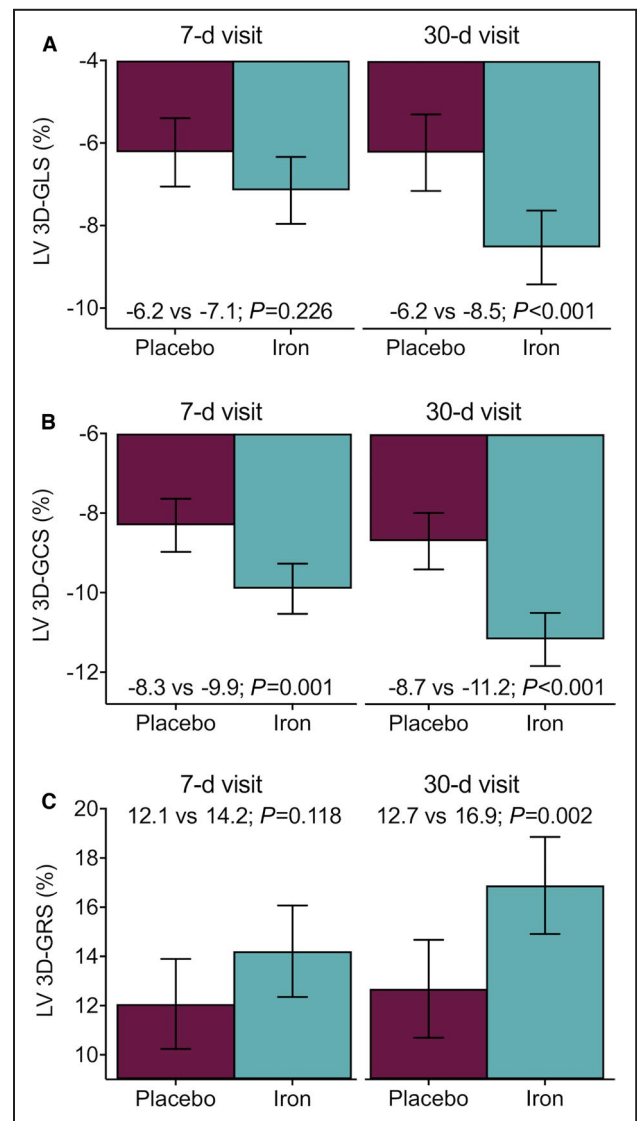


Figure 2. Differences in left ventricular (LV) strain on cardiac magnetic resonance feature tracking at 7 and 30 days following the administration of ferric carboxymaltose in patients included in the Myocardial-IRON trial.

Values are presented as the least square means from each linear mixed model. All models were adjusted by the participant center (as a cluster variable), the interaction term treatment visit (7 and 30 days), age, sex, and the baseline (pretreatment) value of the regressed outcome. (A) LV 3D-GLS. (B) LV 3D-GCS. (C) LV 3D-GRS. 3D-GCS indicates 3-dimensional global circumferential strain; 3D-GLS, 3-dimensional global longitudinal strain; and 3D-GRS, 3-dimensional global radial strain.

RV 2D-GRS

Observed means of RV 2D-GRS in the 2 study groups are presented in Table 2. Likewise, prior RV strain parameters, we could not find different significant values at 7 days (difference: 0.8%; 95% CI, -3.2 to 4.9; $P=0.870$). On the contrary, 2D-GRS were significantly higher in the active arm at 30 days (difference: 4.5%; 95% CI, 0.4 to 8.6; $P=0.027$) (Figure 3C).

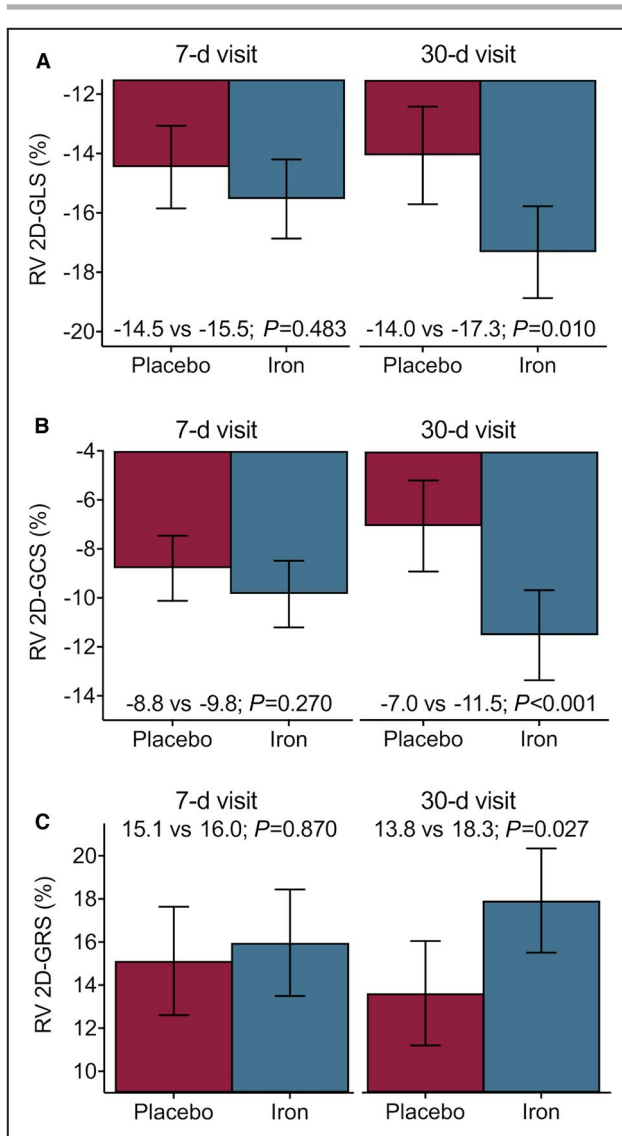


Figure 3. Differences in right ventricular (RV) strain on cardiac magnetic resonance feature tracking at 7 and 30 days following the administration of ferric carboxymaltose in patients included in the Myocardial-IRON trial.

Values are presented as the least square means from each linear mixed effects model. All models were adjusted by the participant center (as a cluster variable), the interaction term treatment*visit (7 and 30 days), age, sex, and the baseline (pretreatment) value of the regressed outcome. (A) RV 2D-GLS. (B) RV 2D-GCS. (C) RV 2D-GRS. 2D-GCS indicates 2-dimensional global circumferential strain; 2D-GLS, 2-dimensional global longitudinal strain; and 2D-GRS, 2-dimensional global radial strain.

Association Between LV CMR-FT Strain Parameters and Changes in T2*, TSAT, and Ferritin

Correlations among changes in LV CMR-FT strain parameters and changes in T2* at 30 days are presented in Table S4. In treated patients, changes in LV 3D-GRS and T2* were significant ($r=-0.42$, $P=0.045$). Other correlations were not significant. In an inferential analysis,

the relationship between the increase in LV 3D-GRS and decreased T2* in those allocated to the active-arm remained statistically significant (Figure 4).

Correlations among 30-day changes in LV CMR-FT strain parameters and 30-day changes in ferrokinetic parameters were not significant (Table S4).

Iron Treatment and Changes in LV- and RV-Strain by Cardiac Magnetic Resonance Feature Tracking in Those With LVEF $\leq 40\%$

Similar findings were found in a sensitivity analysis, including only patients with LVEF $\leq 40\%$ ($n=27$). Most of the strain parameters tested in the active arm improved at 30 days (Figure S1).

Inter-Observer Reproducibility

Inter-observer reproducibility was good to excellent for all analyzed strain measures. Regarding measurements of LV strain, intraclass correlation coefficient values (and their 95% CI) were 0.928 (0.852–0.966), 0.959 (0.902–0.981) and 0.923 (0.846–0.963) for GLS, GCS, and GRS, respectively. For measurements of RV strain, intraclass correlation coefficient values were 0.912 (0.813–0.959), 0.958 (0.906–0.981) and 0.955 (0.902–0.979) for GLS, GCS, and GRS, respectively.

DISCUSSION

To the best of our knowledge, this is the first report showing that iron repletion resulted in a significant short-term improvement of LV- and RV-CMR-FT strain parameters in patients with chronic HF with LVEF $< 50\%$ and ID (Figure 5).

Iron Deficiency and Myocardial Function

Iron is a crucial element required for a wide range of cellular processes, as a component of the active site of many enzymes (mitochondrial respiratory chain, oxidative enzymes), oxygen transport (hemoglobin), and storage (myoglobin).^{1,9–11} Previous experimental investigations have demonstrated that iron deficiency affects cardiomyocytes' function by impairing mitochondrial respiration morphology, ATP production, and contractility.^{9–11} In a clinical setting, ID has been described as frequent comorbidity in HF, affecting between 40% to 80% of patients.^{1,2,27,28} It is mainly associated with decreased functional capacity and a higher risk of adverse outcomes in patients with LV systolic dysfunction.^{1,2,27,28} The data endorsing the role of ID in the pathophysiology of pulmonary vascular remodeling and RV HF is more scarce. However, there is also experimental and clinical data linking ID with pulmonary hypertension and RV HF.^{29–32} For instance, in a

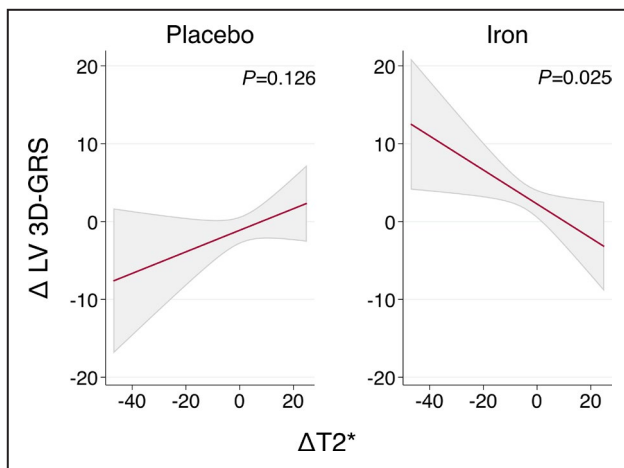


Figure 4. Association of left ventricular 3D-global radial strain with changes in myocardial iron content (T2*).

Values are the least-square means (95% CIs) from each linear regression analysis. LV 3D-GRS indicates left ventricular 3-dimensional global radial strain.

recent study from our group in 903 patients admitted with acute decompensated heart failure, we found that proxies of ID were significantly associated with echocardiographic parameters of RV dysfunction.³²

Iron Repletion and Changes in Ventricular Systolic Function

In an experimental field, iron repletion can reverse ID-related myocardial morphological and functional abnormalities.¹¹ In the clinical setting, important clinical trials have consistently shown that administration of FCM in patients with HF and LVEF <50% is associated with a significant improvement in functional capacity, quality of life, and reduction of rehospitalizations.³⁻⁷ However, notwithstanding the rising proofs and investigations on the benefits of iron treatment in HF, there is limited clinical data on the direct mechanism explaining these findings. Specifically, there is scarce and heterogeneous evidence endorsing the effect of iron repletion on systolic ventricular function.³³⁻³⁵ For instance, some clinical trials have reported that iron therapy improves LVEF and echocardiographic parameters of right ventricular systolic function.^{33,34} However, other studies have failed to find significant changes in LVEF after iron supplementation.^{12,35} Likewise, in the Myocardial-IRON trial, we could not see a significant short-term improvement of CMR-LVEF in the whole sample following the administration of FCM.¹² However, a secondary analysis conducted in patients with greater systolic dysfunction at baseline, FCM was associated with significant short-term improvements in LVEF and RV ejection fraction assessed by CMR.³⁶

More accurate imaging-based techniques, such as myocardial strain analyses, have developed to

overcome the limitation of traditional echocardiographic parameters for evaluating systolic myocardial function (high variability and reproducibility of measurements, and the load-dependence).¹³ Additionally, it is also worth mentioning that conventional echocardiographic parameters for RV function also have well-recognized limitations.

In this regard, CMR feature tracking has emerged as a novel technique that allows accurate, non-invasive, and reproducible cardiac deformation parameters assessment.¹⁶ This is especially true for evaluating RV function in which CMR provides a precise evaluation of RV geometry and function.³⁷ There are not previous well-controlled studies assessing the effect of iron supplementation on strain parameters. In an open-label 1-arm survey, Gaber et al showed in 40 patients with LVEF <40% and ID that iron correction with iron dextran did not significantly increase LVEF but improved peak systolic strain assessed by echocardiography.³⁵ In the current analysis of a double-blind controlled randomized clinical trial, we found significant improvement in CMR-FT derived LV and RV GLS, GCS, and GRS at 30 days after treatment with FCM. The Myocardial-IRON trial's main results showed that following FCM administration, there were CMR changes suggestive of myocardial repletion. The results of this subanalysis may help disentangle part of the short-term myocardial mechanisms behind the clinical benefits related to iron repletion therapy in HF.

There are important issues that remain to be clarified. For instance, we should require more information about the accuracy of T2* and T1-mapping changes as proxies of myocardial iron repletion and prediction of ventricular systolic improvement. Additionally, we should clarify the mid- and long-term effect of FCM on systolic function and whether the increase in right ventricular function is secondary to the improvement of LV or pulmonary hemodynamic or reflects primary changes in right myocardial performance need to be clarified in further studies.

Limitations

Several limitations of our study should be mentioned. First, we cannot evaluate the correlation between CMR feature tracking strain changes and changes in myocardial energetics with the present data. Second, these findings apply to a selected population with stable HF and LVEF <50%, without cardiac devices. Third, the rate of treatment with angiotensin-converting enzyme inhibitors, angiotensin receptor blockers, or angiotensin receptor neprilysin inhibitors were lower than found in recent registries and clinical trials. Probably, the fact that 48% of the patients showed LVEF between 41% to 49% might explain this finding. Fourth, although image quality was good in general, in some patients, difficulty

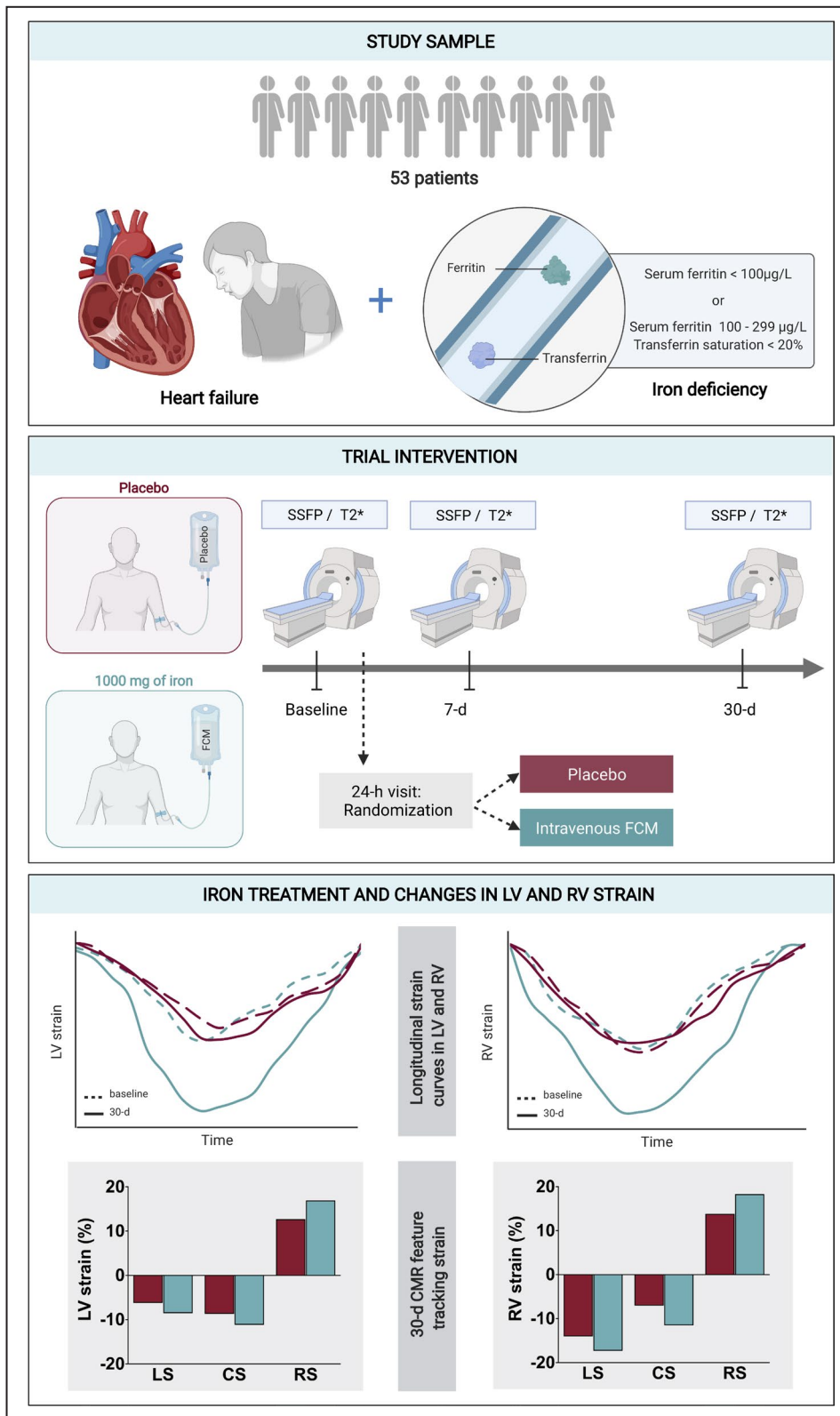


Figure 5. Overview for the short-term improvements in left and right ventricular function, assessed by cardiac magnetic resonance feature tracking derived strain parameters, on patients with stable heart failure and iron deficiency after treatment with ferric carboxymaltose.

CMR indicates cardiac magnetic resonance; CS, circumferential strain; FCM, ferric carboxymaltose; LS, longitudinal strain; LV, left ventricular; RS, radial strain; RV, right ventricular; and SSFP, steady-state free precession.

with long breath-holds was overcome by slightly lowering the spatial resolution. Finally, this is a small study subjected to limited statistical power.

CONCLUSIONS

In this post hoc analysis of the Myocardial-IRON trial on patients with stable HF and ID, treatment with FCM was associated with short-term improvements in LV and RV function assessed by CMR-FT-derived strain parameters. Further investigations should confirm these findings and evaluate the clinical implications derived from them.

APPENDIX

Myocardial Iron Study Group Investigators

Cardiology Department, Hospital Clínico Universitario de Valencia, Universitat de Valencia, INCLIVA, Valencia, Spain: Julio Núñez, MD, PhD, Enrique Santas MD, PhD, Gema Miñana, MD, PhD, Patricia Palau, MD, PhD, Martina Amiguet, MD, Jessika González, MD, Ernesto Valero, MD, Sergio García-Blas, MD, Vicent Bodí, MD, PhD, Rafael de la Espriella-Juan, MD, Jorge Navarro, MD, PhD, Juan Sanchis, MD, PhD, Francisco JChorro, MD, PhD, Meritxell Soler, MD, Amparo Villaescusa, Jose Civera, Anna Mollar, PhD.

Cardiology Department, Hospital General de Castellón. Universitat Jaume I, Castellón, Spain: Alicia Serrano, MD.

Internal Medicine Department, Hospital Ramón y Cajal, Madrid, Spain: Pau Llácer, MD, PhD.

Internal Medicine Department, Hospital de Manises, Manises, Spain: Maria del Carmen Moreno, MD.

Cardiology Department, Hospital de Manises, Manises, Spain: Ingrid Cardells, MD, PhD.

Cardiology Department, Hospital General Universitario de Valencia, Valencia, Spain: Lorenzo Fácila, MD, PhD, Vicente Montagud, MD, Veronica Vidal, MD.

Cardiology Department, Hospital Universitario La Fe de Valencia, Valencia, Spain: Luis Almenar, MD, PhD, Raquel López-Vilella, MD.

ARTICLE INFORMATION

Received April 25, 2021; accepted January 6, 2022.

Affiliations

Cardiology Department, Hospital Clínico Universitario de Valencia, Universitat de Valencia, INCLIVA, Valencia, Spain (I.d.C., E.S., G.M., P.P., V.B., J.S., R.d.I.E., F.J.C., J.N.); CIBER Cardiovascular, Madrid, Spain (I.d.C., E.S., G.M., P.P., V.B., J.S., R.d.I.E., F.J.C., A.B.-G., J.N.); Center for Biomaterials and Tissue Engineering, Universitat Politècnica de València, Valencia, Spain (I.d.C., D.M.); Cardiology Department (I.C.), and Internal Medicine Department (P.L.), Hospital de Manises, Manises, Spain; Cardiology Department, Hospital General Universitario de Valencia, Valencia, Spain (L.F.); Cardiology Department, Hospital Universitario La Fe de Valencia, Valencia, Spain (R.L.-V.,

L.A.); Cardiovascular Imaging Unit, Ascires Biomedical Group, Valencia, Spain (M.P.L.-L., J.V.M., A.M.M.); Cardiology Department and Heart Failure Unit, Hospital Universitari Germans Trias i Pujol, Badalona, Spain (A.B.-G.); and Universitat Autònoma de Barcelona, Barcelona, Spain (A.B.-G.).

Acknowledgment

The authors would like to acknowledge the work of the Clinical Research and Clinical Trials Unit (UICEC INCLIVA).

Sources of Funding

This work was supported in part by an unrestricted grant from Vifor Pharma, CIBER Cardiovascular [grant numbers 16/11/00420 and 16/11/00403], Unidad de Investigación Clínica y Ensayos Clínicos INCLIVA Health Research Institute, Spanish Clinical Research Network (SCReN; PT13/0002/0031 and PT17/0017/0003), cofounded by Fondo Europeo de Desarrollo Regional—Instituto de Salud Carlos III, and Proyectos de Investigación de la Sección de Insuficiencia Cardíaca 2017 from Sociedad Española de Cardiología.

Disclosures

J. Núñez received board speaker fees and travel expenses from Novartis, Roche Diagnostics, Abbott, Rovi, Vifor Pharma, Daiichi Sankyo, Novonordisk, Boehringer Ingelheim, and AstraZeneca (modest). L. Fácila received speaker fees and travel expenses from Novartis (modest). Juan Sanchis received speaker fees from Astra-Zeneca, Abbott, and Edwards Lifesciences (modest). A. Bayés-Genís received board membership fees and travel expenses from Novartis, Roche Diagnostics, Vifor Pharma, and Critical Diagnostics (modest). The remaining authors have no disclosures to report.

Supplemental Material

Tables S1–S4

Figure S1

REFERENCES

1. Rocha BML, Cunha GJL, Menezes Falcao LF. The burden of iron deficiency in heart failure: therapeutic approach. *J Am Coll Cardiol*. 2018;71:782–793. doi: 10.1016/j.jacc.2017.12.027
2. Núñez J, Comin-Colet J, Miñana G, Núñez E, Santas E, Mollar A, Valero E, García-Blas S, Cardells I, Bodí V, et al. Iron deficiency and risk of early readmission following a hospitalization for acute heart failure *Eur J Heart Fail*. 2016;18:798–802. doi: 10.1002/ehf.513
3. Ponikowski P, Voors AA, Anker SD, Bueno H, Cleland JGF, Coats AJS, Falk V, González-Juanatey JR, Harjola V-P, Jankowska EA, et al. 2016 ESC guidelines for the diagnosis and treatment of acute and chronic heart failure: the Task Force for the diagnosis and treatment of acute and chronic heart failure of the European Society of Cardiology (ESC). Developed with the special contribution of the Heart Failure Association (HFA) of the ESC. *Eur J Heart Fail*. 2016;18:891–975. doi: 10.1002/ehf.592
4. Anker SD, Comin Colet J, Filippatos G, Willenheimer R, Dickstein K, Drexler H, Lüscher TF, Bart B, Banasiak W, Niegowska J, et al; FAIR-HF Trial Investigators. Ferric carboxymaltose in patients with heart failure and iron deficiency. *N Engl J Med*. 2009;361:2436–2448. doi: 10.1056/NEJMoa0908355
5. Ponikowski P, van Veldhuisen DJ, Comin-Colet J, Ertl G, Komajda M, Mareev V, McDonagh T, Parkhomenko A, Tavazzi L, Levesque V, et al; CONFIRM-HF Investigators. Beneficial effects of long-term intravenous iron therapy with ferric carboxymaltose in patients with symptomatic heart failure and iron deficiency. *Eur Heart J*. 2015;36:657–668. doi: 10.1093/eurheartj/ehu385
6. Anker SD, Kirwan B-A, van Veldhuisen DJ, Filippatos G, Comin-Colet J, Ruschitzka F, Lüscher TF, Arutyunov GP, Motro M, Mori C, et al. Effects of ferric carboxymaltose on hospitalisations and mortality rates in iron-deficient heart failure patients: an individual patient data meta-analysis. *Eur J Heart Fail*. 2018;20:125–133. doi: 10.1002/ehf.823
7. Ponikowski P, Kirwan B-A, Anker SD, McDonagh T, Dorobantu M, Drozd J, Fabien V, Filippatos G, Göhring UM, Keren A, et al. Ferric carboxymaltose for iron deficiency at discharge after acute heart failure: a multicentre, double-blind, randomised, controlled trial. *Lancet*. 2020;396:1895–1904. doi: 10.1016/S0140-6736(20)32339-4
8. Ghafourian K, Chang HC, Ardehali H. Intravenous iron therapy in heart failure: a different perspective. *Eur J Heart Fail*. 2019;21:703–714. doi: 10.1002/ehf.1434

9. Ghafourian K, Shapiro JS, Goodman L, Ardehali H. Iron and heart failure. *J Am Coll Cardiol Basic Trans Sci.* 2020;5:300–313.
10. Kobak KA, Radwańska M, Dziegala M, Kasztura M, Josiak K, Banasiak W, Ponikowski P, Jankowska EA. Structural and functional abnormalities in iron-depleted heart. *Heart Fail Rev.* 2019;24:269–277. doi: 10.1007/s10741-018-9738-4
11. Hoes MF, Grote Beverborg N, Kijlstra JD, Kuipers J, Swinkels DW, Giepmans BNG, Rodenburg RJ, van Veldhuisen DJ, de Boer RA, van der Meer P. Iron deficiency impairs contractility of human cardiomyocytes through decreased mitochondrial function. *Eur J Heart Fail.* 2018;20:910–919. doi: 10.1002/ehf.1154
12. Nuñez J, Minana G, Cardells I, Palau P, Llacer P, Facila L, Almenar L, Lopez-Lereu MP, Monmeneu JV, Amiguet M, Myocardial-IRON Investigators, et al. Non-invasive imaging estimation of myocardial iron repletion following administration of intravenous iron: the myocardial-IRON Trial. *J Am Heart Assoc.* 2020;9:e014254. doi: 10.1161/JAHA.119.014254
13. Halliday BP, Senior R, Pennell DJ. Assessing left ventricular systolic function: from ejection fraction to strain analysis. *Eur Heart J.* 2021;42:789–797. doi: 10.1093/eurheartj/ehaa587
14. Choi E-Y, Rosen BD, Fernandes VRS, Yan RT, Yoneyama K, Donekal S, Opdahl A, Almeida ALC, Wu CO, Gomes AS, et al. Prognostic value of myocardial circumferential strain for incident heart failure and cardiovascular events in asymptomatic individuals: the Multi-Ethnic Study of Atherosclerosis. *Eur Heart J.* 2013;34:2354–2361. doi: 10.1093/eurheartj/ehs133
15. Cho GY, Marwick TH, Kim HS, Kim MK, Hong KS, Oh DJ. Global 2-dimensional strain as a new prognosticator in patients with heart failure. *J Am Coll Cardiol.* 2009;54:618–624. doi: 10.1016/j.jacc.2009.04.061
16. Scatteia A, Baritussio A, Bucciarelli-Ducci C. Strain imaging using cardiac magnetic resonance. *Heart Fail Rev.* 2017;22:465–476. doi: 10.1007/s10741-017-9621-8
17. Schuster A, Hor KN, Kowalick JT, Beerbaum P, Kutty S. Cardiovascular magnetic resonance myocardial feature tracking. *Circ Cardiovasc Imaging.* 2016;9:e004077. doi: 10.1161/CIRCIMAGING.115.004077
18. Miñana G, Cardells I, Palau P, Llacer P, Fácila L, Almenar L, López-Lereu MP, Monmeneu JV, Amiguet M, González J, et al. Myocardial-IRON investigators. Changes in myocardial iron content following administration of intravenous iron (Myocardial-IRON): study design. *Clin Cardiol.* 2018;41:729–735. doi: 10.1002/clc.22956
19. Ponikowski P, Voors AA, Anker SD, Bueno H, Cleland JGF, Coats AJS, Falk V, González-Juanatey JR, Harjola V-P, Jankowska EA, et al. ESC Scientific Document Group. 2016 ESC guidelines for the diagnosis and treatment of acute and chronic heart failure: the Task Force for the diagnosis and treatment of acute and chronic heart failure of the European Society of Cardiology (ESC) Developed with the special contribution of the Heart Failure Association (HFA) of the ESC. *Eur Heart J.* 2016;37:2129–2200. doi: 10.1093/eurheartj/ehw128
20. Nutritional anaemias. *Report of a WHO scientific group.* Geneva: World Health Organization; 1968. (WHO Technical Report Series, No. 405).
21. Weintraub WS, Karlsberg RP, Tchong JE, Boris JR, Buxton AE, Dove JT, Fonarow GC, Goldberg LR, Heidenreich P, Hendel RC, et al. ACCF/AHA 2011 key data elements and definitions of a base cardiovascular vocabulary for electronic health records: a report of the American College of Cardiology Foundation/American Heart Association Task Force on Clinical Data Standards. *J Am Coll Cardiol.* 2011;58:202–222. doi: 10.1016/j.jacc.2011.05.001
22. Gatti M, Palmisano A, Falletti R, Benedetti G, Bergamasco L, Bioletto F, Peretto G, Sala S, De Cobelli F, Fonio P, et al. Two-dimensional and three-dimensional cardiac magnetic resonance feature-tracking myocardial strain analysis in acute myocarditis patients with preserved ejection fraction. *Int J Cardiovasc Imaging.* 2019;35:1101–1109. doi: 10.1007/s10554-019-01588-8
23. Liu B, Dardeer AM, Moody WE, Hayer MK, Biag S, Price AM, Leyva F, Edwards NC, Steeds RP. Reference ranges for three-dimensional feature tracking cardiac magnetic resonance: comparison with two-dimensional methodology and relevance of age and gender. *Int J Cardiovasc Imaging.* 2018;34:761–775. doi: 10.1007/s10554-017-1277-x
24. Schmidt B, Dick A, Treutlein M, Schiller P, Bunck AC, Maintz D, Baeßler B. Intra- and inter-observer reproducibility of global and regional magnetic resonance feature tracking derived strain parameters of the left and right ventricle. *Eur J Radiol.* 2017;89:97–105. doi: 10.1016/j.ejrad.2017.01.025
25. He T. Cardiovascular magnetic resonance T2* for tissue iron assessment in the heart. *Quant Imaging Med Surg.* 2014;4:407–412. doi: 10.3978/j.issn.2223-4292.2014.10.05
26. Jakobsen JC, Gluud C, Wetterslev J, Winkel P. When and how should multiple imputation be used for handling missing data in randomised clinical trials - a practical guide with flowcharts. *BMC Med Res Methodol.* 2017;17:162. doi: 10.1186/s12874-017-0442-1
27. Klip IT, Comin-Colet J, Voors AA, Ponikowski P, Enjuanes C, Banasiak W, Lok DJ, Rosentryt P, Torrens A, Polonski L, et al. Iron deficiency in chronic heart failure: an international pooled analysis. *Am Heart J.* 2013;165:575–582.e573. doi: 10.1016/j.ahj.2013.01.017
28. von Haehling S, Gremmler U, Krumm M, Mibach F, Schon N, Taggeselle J, Dahm JB, Angermann CE. Prevalence and clinical impact of iron deficiency and anaemia among outpatients with chronic heart failure: the PREP Registry. *Clin Res Cardiol.* 2017;106:436–443. doi: 10.1007/s00392-016-1073-y
29. Leszek P, Sochanowicz B, Szperl M, Kolsut P, Brzóška K, Piotrowski W, Rywik TM, Danko B, Polkowska-Motrenko H, Różański JM, et al. Myocardial iron homeostasis in advanced chronic heart failure patients. *Int J Cardiol.* 2012;159:47–52. doi: 10.1016/j.ijcard.2011.08.006
30. Alioglu B, Cetin II, Emeksiz ZS, Dindar N, Tapci E, Dallar Y. Iron deficiency anemia in infants: does it really affect the myocardial functions? *Pediatr Hematol Oncol.* 2013;30:239–245. doi: 10.3109/0888018.2012.763077
31. Cotroneo E, Ashek A, Wang L, Wharton J, Dubois O, Bozorgi S, Busbridge M, Alavian KN, Wilkins MR, Zhao L. Iron homeostasis and pulmonary hypertension: iron deficiency leads to pulmonary vascular remodeling in the rat. *Circ Res.* 2015;116:1680–1690. doi: 10.1161/CIRCRESAHA.116.305265
32. Miñana G, Santas E, de la Espriella R, Núñez E, Lorenzo M, Núñez G, Valero E, Bodí V, Chorro FJ, Sanchis J, et al. Right ventricular function and iron deficiency in acute heart failure. *Eur Heart J Acute Cardiovasc Care.* 2021;10:406–414. doi: 10.1093/ehjacc/zuaa028
33. Parissis JT, Kourea K, Panou F, Farmakis D, Paraskevidis I, Ikonomidis I, Filippatos G, Kremastinos DT. Effects of darbepoetin alpha on right and left ventricular systolic and diastolic function in anemic patients with chronic heart failure secondary to ischemic or idiopathic dilated cardiomyopathy. *Am Heart J.* 2008;155:e751–e757. doi: 10.1016/j.ahj.2008.01.016
34. Toblli JE, Di Gennaro F, Rivas C. Changes in echocardiographic parameters in iron deficiency patients with heart failure and chronic kidney disease treated with intravenous iron. *Heart Lung Circ.* 2015;24:686–695. doi: 10.1016/j.hlc.2014.12.161
35. Gaber R, Kotb NA, Ghazy M, Nagy HM, Salama M, Elhendy A. Tissue Doppler and strain rate imaging detect improvement of myocardial function in iron deficient patients with congestive heart failure after iron replacement therapy. *Echocardiography.* 2012;29:13–18. doi: 10.1111/j.1540-8175.2011.01532.x
36. Santas E, Miñana G, Cardells I, Palau P, Llacer P, Fácila L, Almenar L, López-Lereu MP, Monmeneu JV, Sanchis J, et al; Myocardial-IRON Investigators. Short-term changes in left and right systolic function following ferric carboxymaltose: a substudy of the Myocardial-IRON trial. *ESC Heart Fail.* 2020;7:4222–4230. doi: 10.1002/ehf2.13053
37. Badano LP, Addetia K, Pontone G, Torlasco C, Lang RM, Parati G, Muraru D. Advanced imaging of right ventricular anatomy and function. *Heart.* 2020;106:1469–1476. doi: 10.1136/heartjnl-2019-315178

SUPPLEMENTAL MATERIAL

Table S1. Details of performed sequences for CMR acquisition

CMR sequence parameters	Cine	T2*
Pulse sequence	SSFP	Multiecho gradient
Slice thickness	7 mm	8 mm
Field of view	400 x 300	400 x 324
Matrix size	240 x 240	256 x 154
Slice oversampling	No	No
Voxel size	1.7 x 1.7 x 7 mm	1.6 x 1.6 x 8 mm
Echo time	1.41 ms	Ascending (2.65 to 21 ms)
Repeat time	37.40 ms	800 ms
Flip angle	58°	20°
Bandwidth (Hz/Px)	947	814
Acceleration	GRAPPA (x2) No compressed-sensing	GRAPPA (x2) No compressed-sensing

GRAPPA: Generalized autocalibrating partially parallel acquisition

Table S2. CMR feature tracking LV strain models

LV 3D-GLS	Coeff.	95% CI	p-value
Covariates			
LV 3D-GLS at baseline	0.53	0.39 - 0.67	0.000
Age (years) at baseline	-0.04	-0.10 - 0.01	0.124
Sex	-0.38	-1.64 - 0.89	0.560
1.iron_tx	-0.92	-2.09 - 0.24	0.120
2.visit	-0.00	-0.86 - 0.85	0.995
1.iron_tx#2.visit	-1.38	-2.56 - -0.19	0.023
N	97		
LV 3D-GCS	Coeff.	95% CI	p-value
Covariates			
LV 3D-GCS at baseline	0.81	0.69 - 0.93	0.000
Age (years) at baseline	0.02	-0.02 - 0.06	0.369
Sex	0.44	-0.51 - 1.39	0.364
1.iron_tx	-1.59	-2.51 - -0.68	0.001
2.visit	-0.39	-1.22 - 0.44	0.361
1.iron_tx#2.visit	-0.88	-2.02 - 0.25	0.128
N	100		
LV 3D-GRS	Coeff.	95% CI	p-value
Covariates			
LV 3D-GRS at baseline	0.59	0.42 - 0.77	0.000
Age (years) at baseline	0.02	-0.08 - 0.12	0.728
Sex	-0.89	-3.01 - 1.23	0.410
1.iron_tx	2.14	-0.10 - 4.38	0.061
2.visit	0.63	-1.62 - 2.88	0.584
1.iron_tx#2.visit	2.07	-1.06 - 5.20	0.194
N	97		

LV 3D-GLS: left ventricle 3D-global longitudinal strain; LV 3D-GCS: left ventricle 3D-global circumferential strain; LV 3D-GRS: left ventricle 3D-global radial strain.

Table S3. CMR feature tracking RV strain models

RV 2D-GLS	Coeff.	95% CI	p-value
Covariates			
RV 2D-GLS at baseline	0.76	0.59 - 0.93	0.000
Age (years) at baseline	-0.00	-0.10 - 0.09	0.947
Sex	1.02	-1.01 - 3.05	0.326
1.iron_tx	-1.07	-3.03 - 0.88	0.281
2.visit	0.41	-1.24 - 2.05	0.627
1.iron_tx#2.visit	-2.19	-4.45 - 0.07	0.057
N	97		
RV 2D-GCS	Coeff.	95% CI	p-value
Covariates			
RV 2D-GCS at baseline	0.73	0.58 - 0.88	0.000
Age (years) at baseline	-0.07	-0.14 - 0.01	0.075
Sex	0.45	-1.09 - 1.99	0.568
1.iron_tx	-1.05	-2.47 - 0.36	0.145
2.visit	1.74	-0.02 - 3.50	0.052
1.iron_tx#2.visit	-3.42	-5.86 - -0.98	0.006
N	101		
RV 2D-GRS	Coeff.	95% CI	p-value
Covariates			
RV 2D-GRS at baseline	0.46	0.29 - 0.63	0.000
Age (years) at baseline	0.08	-0.09 - 0.25	0.367
Sex	0.31	-3.39 - 4.01	0.869
1.iron_tx	0.84	-2.68 - 4.37	0.639
2.visit	-1.30	-3.85 - 1.24	0.315
1.iron_tx#2.visit	3.65	0.08 - 7.22	0.045
N	99		

RV 2D-GLS: right ventricle 2D-global longitudinal strain; RV 2D-GCS: right ventricle 2D-global circumferential strain; RV 2D-GRS: right ventricle 2D-global radial strain.

Table S4. Correlations among 30-day changes LV strain parameters and changes in T2*, TSAT, and ferritin.

	$\Delta T2^*$	$\Delta TSAT$	$\Delta Ferritin$
Iron FCM			
ΔLV 3D-GLS	0.30 (p=0.183)	0.06 (p=0.742)	0.04 (p=0.889)
ΔLV 3D-GCS	0.18 (p=0.426)	0.13 (p=0.561)	-0.21 (p=0.339)
ΔLV 3D-GRS	-0.42 (p=0.045)	-0.08 (p=0.751)	0.21 (p=0.330)
Placebo			
ΔLV 3D-GLS	0.22 (p=0.325)	-0.20 (p=0.401)	0.18 (p=0.436)
ΔLV 3D-GCS	-0.14 (p=0.543)	-0.28 (p=0.231)	0.19 (p=0.414)
ΔLV 3D-GRS	0.23 (p=0.330)	0.33 (p=0.155)	0.13 (p=0.573)

FCM: ferric carboxymaltose; LV 3D-GLS: left ventricle 3D-global longitudinal strain; LV 3D-GCS: left ventricle 3D-global circumferential strain; LV 3D-GRS: left ventricle 3D-global radial strain.

The Spearman test evaluated correlations.

Figure S1. Differences in LV and RV strain on CMR-FT at 7 and 30 days following the administration of ferric carboxymaltose in patients with baseline LVEF \leq 40%. Values are presented as the least square means from each mixed linear regression model. All models were adjusted by the participant center (as a cluster variable), the interaction term treatment*visit (7 and 30 days), age, sex, and the baseline (pretreatment) value of the regressed outcome. (A) LV 3D-global longitudinal strain (LV 3D-GLS). (B) LV 3D-global circumferential strain (LV 3D-GCS). (C) LV 3D-global radial strain (LV 3D-GRS). (D) RV 2D-global longitudinal strain (RV 2D-GLS). (E) RV 2D-global circumferential strain (RV 2D-GCS). (F) RV 2D-global radial strain (RV 2D-GRS). CMR-FT: cardiac magnetic resonance feature tracking.

